AEROELASTIC PREDICTION FOR MISSILE FINS IN SUPERSONIC FLOWS

Marius-Corné Meijer
University of the Witwatersrand
mariuscmeijer@gmail.com

Keywords: *aeroelasticity, piston theory, flutter prediction, zero-order*

Abstract

The development of a zero-order aeroelastic prediction method for plate-like structures in supersonic flows is outlined. Local piston theory used with computationally inexpensive aerodynamic methods is strongly coupled to a simple finite element code for plates to produce a partitioned-solver aeroelastic prediction tool. The application of the prediction tool to the flutter of a cantilevered plate in supersonic flow is validated by computational fluid dynamics and by experimental data in literature. The zero-order prediction method is shown to produce accurate results for a fraction of the computational cost of high-fidelity analysis.

A brief review of piston theory is also given.

1 Introduction

Prediction of the aeroelastic behaviour of lifting and control surfaces at high flow velocities is important from the perspective of both design optimization as well as safe testing of designs. The onset of flutter may be very sudden, and may lead to the rapid destruction of the lifting surface [1] - this sharp onset of flutter is known as “hard” flutter.

A number of codes for aeroelastic modelling and prediction of various analysis fidelities are commercially available [2], ranging from panel methods to coupled finite volume and finite element codes. The only open source code for supersonic aeroelastic analysis readily found was FreeCASE [3]. FreeCASE is a high-fidelity finite volume code for transonic aeroservoelastic computations. High-fidelity aeroelastic analysis by finite volume codes is computationally expensive, which may render it unsuitable for parametric design studies, or prohibitive to implement in the design of experiments.

In this paper, the development and application of a zero-order method for aeroelastic modelling and computational flutter prediction is outlined. The method is based on the use of local piston theory with computationally inexpensive methods for steady aerodynamic analysis. A partitioned solver is employed with strong coupling between the aerodynamic method and a basic finite element code. The resulting prediction tool is shown to be suitably accurate for preliminary modelling, and is shown to be capable of predicting hard flutter.

2 Piston Theory

2.1 Literature Review

Piston theory is an analytical method that gives a point-function expression for the aerodynamic pressure on the surface of a body in supersonic flow. The body surface is treated as a piston moving in a 1-D cylinder transverse to the flow direction, as illustrated in Fig. 1. The pressure is modelled from the upwash on the face of the piston. It is a quasi-steady, local theory in which the pressure is a function of only the local downwash [4]. It may also be seen to be an application of the hypersonic equivalence principle between 2-D steady flow and 1-D unsteady flow [5].

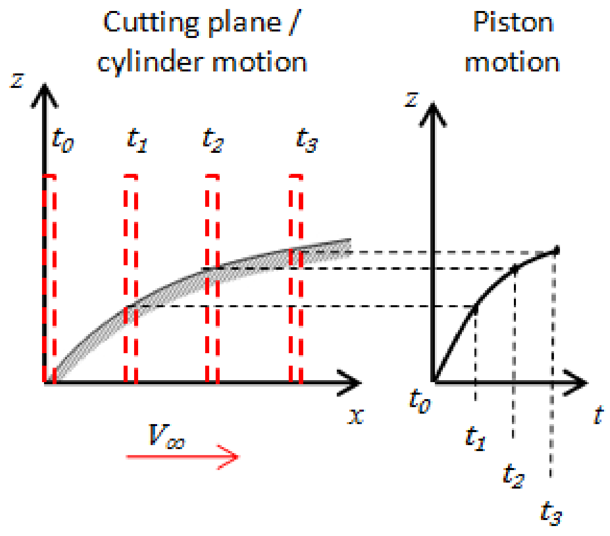

Fig. 1 : Piston theory terminology.

The original development of piston theory is generally accredited to Lighthill [6]. In the original formulation, the pressure at a point on a body due to both steady and unsteady aerodynamic contributions was solved for; this will be referred to as "classical piston theory" (CPT). Lightill's pressure formulation was based on the equations of 1-D compressible flow for a piston generating isentropic simple waves [7]. The limits of validity were established by Ashley and Zartarian [7] as flows for which $M \gg 1$, $kM^2 \gg 1$, or $k^2M^2 \gg 1$, where k is the reduced frequency of oscillation and M is the Mach number of the flow. Furthermore, the analysis was limited to bodies with sharp leading and trailing edges with attached shocks.

Further developments to piston theory were reviewed by Liu et al [8], who also coupled 3rd-order CPT with supersonic lifting surface theory to account for 3-D influence. The review of Liu et al considered the work of previous authors in formulating higher-order piston theories, including Van Dyke's unified supersonic-hypersonic theory [9] and Donov's [10] 4th-order series for the surface pressure. These works assumed that shocks remain attached over the length of the body. Liu et al estimated the range of validity of these works to lie between between $0.368 \leq K \leq 1.05$, where K is the hypersonic similarity parameter defined as in Fig. 2 and represents the upwash Mach number.

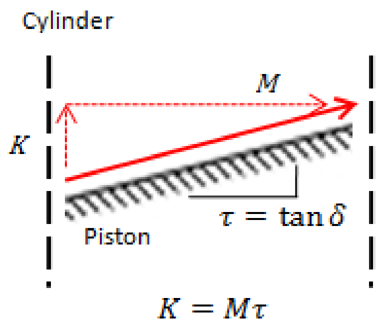

Fig. 2 : Upwash Mach number in piston theory.

An important development in piston theory was made by Zhang et al [11], in which 1st-order piston theory was used to analyse only the unsteady contribution to pressure; this was dubbed "local piston theory" (LPT). In the work of Zhang et al, the mean steady flowfield was solved by computational fluid dynamics (CFD) using steady-state Euler analyis. It was shown [11] that excellent correlation between full unsteady Euler analysis and the steady Euler/LPT could be obtained for small oscillations at Mach numbers in the range $2 \leq M \leq 12$. The use of the Euler code to obtain the steady contribution eliminated restrictions on the airfoil shape that were associated with CPT.

Recently, an extension to linear piston theory and its range of validity was made by Dowell and Bliss [4]. In their treatment, linear piston theory is shown to exist as the first term in an expansion of the equation for pressure from unsteady linear potential flow theory in terms of inverse powers of k or of M^2. The derivation is made assuming simple harmonic motion, and offers an extension of the range of validity for piston theory in terms of both reduced frequency of oscillation and Mach number, as these parameters are factored into the calculation of the coefficients in the extended piston theory.

Piston theory remains an active topic of research and application, with several [12–14] applications made in the field of aerothermoelasticity.

2.2 Fundamental Formulation

The basis for piston theory involves the binomial expansion of an expression for the pressure on a surface, P_{piston}, cast in terms of the local upwash or flow turning angle.

$$\frac{P_{piston}}{P_{cyl}} = 1 + \gamma E \tag{1}$$

where γ is ratio of specific heats of the gas, E denotes the other terms in the binomial expansion, and where the reference pressure P_{cyl} depends on the use of local or classical piston theory. Typically, the expression E is of the form

$$E = c_1 \left(\frac{w}{a_{cyl}}\right) + c_2 \left(\frac{w}{a_{cyl}}\right)^2 + \dots \tag{2}$$

in which c_1, c_2, and higher-order coefficients depend on the equation the expression is based on, w represents the upwash at the point on the body, and a_{cyl} is the reference speed of sound, which depends on the use of local or classical piston theory.

The piston upwash may be expressed as the sum of the contribution arising from steady effects (w_0, such as the body shape and flow incidence) and unsteady effects (w_1, such as body motion)

$$w = w_0 + w_1 \tag{3}$$

where the contributions are defined in Fig. 3

The order of the piston theory applied is based on the order of the upwash term that the expression for pressure (Eqn. 2) is expanded up to. Higher order upwash terms introduce coupling between the steady and unsteady contributions to the upwash. This carries through to increased fidelity of modelling of the pressure. In broad terms [5],

- 1st-order piston theory models linear steady contributions from camber and α, and linear damping,
- 2nd-order piston theory introduces linear thickness effects on the steady and unsteady aerodynamic loads,
- 3rd-order piston theory introduces nonlinear steady effects and damping, and introduces coupling between the steady aerodynamic loading and the damping.

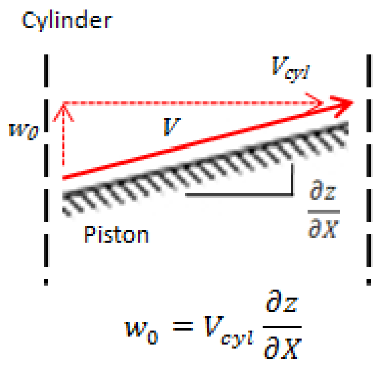

(a) Steady contribution

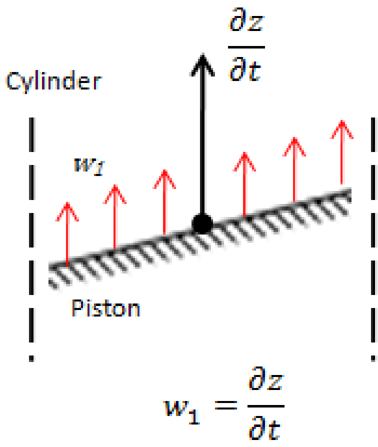

(b) Unsteady contribution

Fig. 3 : Contributions to the piston upwash.

It has been noted by Liu et al [8] that from the third-order terms and higher, differences in the physics of expansion and compression in supersonic flows are modelled in the pressure.

2.3 Classical vs Local Piston Theory

The difference in formulation between LPT and CPT stems from the choice of reference frame for the piston and cylinder [5]. In CPT, the cylinder is in an earth-fixed reference frame through which the body passes, as shown in Fig. 4; the cylinder reference conditions are the ambient conditions of the atmosphere, and the piston motion arises due to body shape, incidence, and motion of the body down the cylinder. As a consequence, both the steady and unsteady contributions to pressure are accounted for.

In LPT, the cylinder reference frame is analogous to the laboratory reference frame for a body mounted in a wind-tunnel, with pitch and plunge motion permitted; piston motion arises due to the motion of the surface of the body down the length of the cylinder, as shown in Fig. 5. The cylinder reference conditions in LPT are taken to be equal to the local steady flow conditions at the point on the body surface under consideration. Only the changes relative to the mean steady state (i.e., unsteady contributions) are modelled.

The cylinder conditions in both classical and local piston theory are assumed to remain constant. In LPT, this essentially results in the dynamic linearization of the flow, as small perturbations about a mean steady flow are assumed.

In summary, the differences in formulation between CPT and LPT are manifested in Eqn. 2 through both the downwash terms (w, w^2, $\dots$) and cylinder reference conditions a_{cyl} and M_{cyl} (which influence the calculation of the coefficients c_1, c_2, $\dots$). In higher-order piston theories, the uncoupled steady downwash terms (w_0, w_0^2, w_o^3, $\dots$) are not used in the calculation of the unsteady pressure in LPT - these terms are accounted for in the steady solution of the flowfield.

The formulation of LPT allows the unsteady pressures due to small vibrations of a body to be computed with a point-function relationship. This renders it a computationally inexpensive method to obtain unsteady aerodynamic loads. The method is also modular in its application, as the only restriction placed on the fidelity of the steady aerodynamic analysis is that the pressure and speed of sound at the body surface must be known.

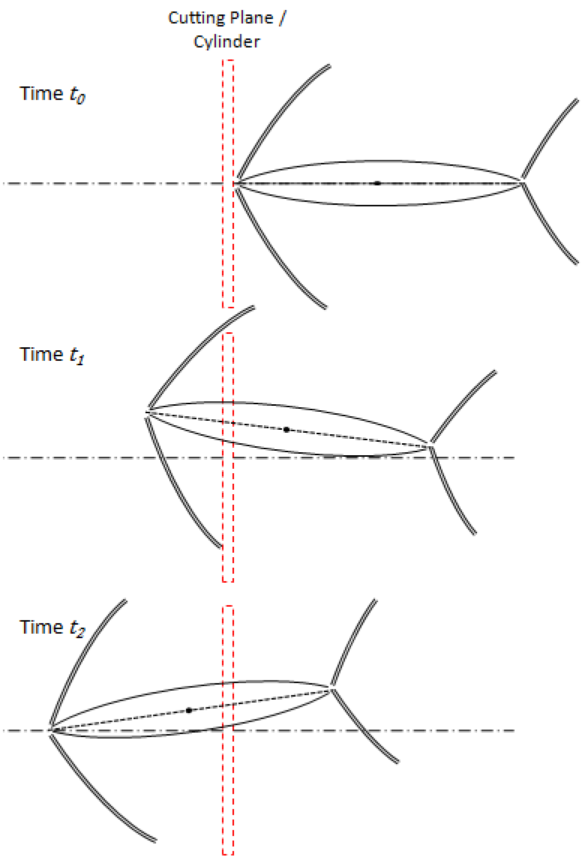

Fig. 4 : Reference frame in CPT.

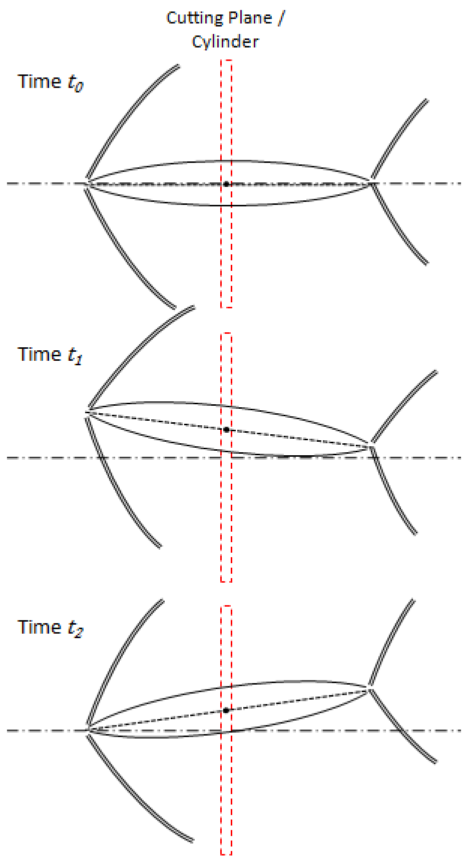

Fig. 5 : Reference frame in LPT.

3 Structural Modelling

In the developed prediction tool of Meijer [5], the structure of a missile fin is modelled as a cantilevered trapezoidal plate with isotropic material properties. A finite element (FE) structural solver was developed using bilinear quadrilateral Mindlin-Reissner bending-plate elements. The FE solver was implemented in MATLAB, and was validated against MSC Nastran for equivalent geometries, meshes, and element type. Linear modal analysis showed agreement to within $\approx 1.5\%$ in modal frequencies between the FE solver and MSC Nastran. Results of the modal analysis of the Torii-Matsuzaki [15] wing (TM-wing) are given in Table 1, with the mode shapes shown in Fig. 6–8 .

Table 1: TM-wing modal frequencies

	Natural frequency, f [Hz]		
Mode	Nastran	MATLAB	Exp. [15]
1	26.6	26.4	27.2
2	148.5	147.7	142.0
3	195.0	192.4	192.3

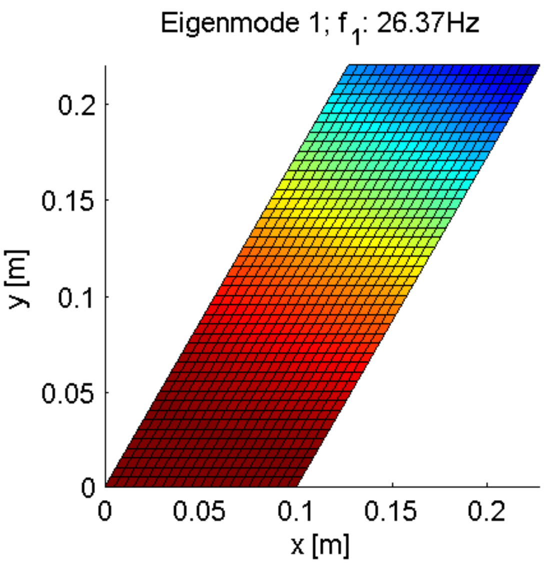

Fig. 6 : TM-wing mode 1: first bending.

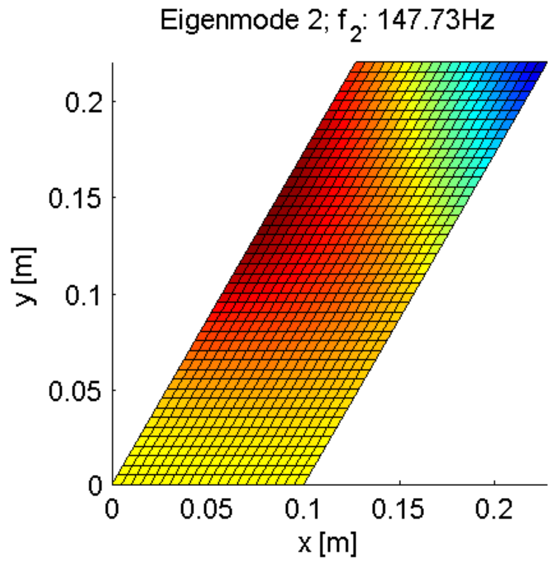

Fig. 7 : TM-wing mode 2: first twisting.

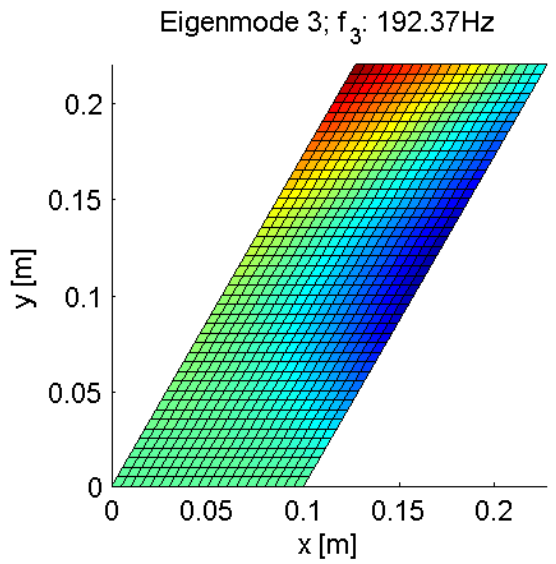

Fig. 8 : TM-wing mode 3: second bending.

4 Aerodynamic Modelling

Third-order local piston theory based on the coefficients of Donov [10] (as deduced by Liu et al [8]) was used in the developed prediction tool to predict the unsteady contribution to the aerodynamic loading. The steady aerodynamic loading was computed using shock-expansion theory along 2-D strips aligned parallel to the root of the fin. This combination of analysis methods will be referred to as

SE/LPT. Implementation of the aerodynamic solver was made in MATLAB. The piston theory coefficients were calculated using the local steady-state conditions from shock-expansion theory (subscript ss), with the unsteady pressure, P_u, calculated as

$$\frac{P_u}{P_{ss}} = 1+\gamma\left[c_1\left(\frac{w}{a_{ss}}\right)+c_2\left(\frac{w}{a_{ss}}\right)^2+c_3\left(\frac{w}{a_{ss}}\right)^3\right] \tag{4}$$

where the coefficients are given by Liu et al [8] as (with $m=\sqrt{M^2-1}$)

$$c_1 = \frac{M_{ss}}{m_{ss}} \tag{5}$$

$$c_2 = \frac{M_{ss}^4(\gamma+1)-4m_{ss}^2}{4m_{ss}^4} \tag{6}$$

$$c_3 = \frac{1}{6M_{ss}m_{ss}^7}\left(aM_{ss}^8+bM_{ss}^6+cM_{ss}^4+dM_{ss}^2+e\right) \tag{7}$$

in which

$$a = \gamma+1 \tag{8}$$

$$b = 2\gamma^2-7\gamma-5 \tag{9}$$

$$c = 10(\gamma+1) \tag{10}$$

$$d = -12 \tag{11}$$

$$e = 8 \tag{12}$$

Shock-expansion theory was chosen for the steady aerodynamic analysis due to its simplicity in implementation, whilst providing the local flow conditions. However, LPT places no restrictions on the steady method used, and as such the use of shock-expansion theory serves as proof of concept of the aeroelastic prediction method. Further work was performed to incorporate steady loading from the supersonic-hypersonic arbitrary-body program (SHABP, Mk IV) into the prediction tool - this was accomplished for the shock-expansion aero option in SHABP, and scope for further integration exists.

The aerodynamic modelling was validated [5] against Euler computations in the Edge CFD code. The computations were performed on the domain shown in Fig. 9. Mesh independence was shown for a tet-dominated unstructured mesh of 1,430,723 elements and 241,879 nodes. The normal force and pitching moment coefficients, predicted using shock-expansion theory in MATLAB for the TM-wing at Mach 3, were found to lie within 5% of the values computed in Edge for the range $0° \leq \alpha \leq 18°$.

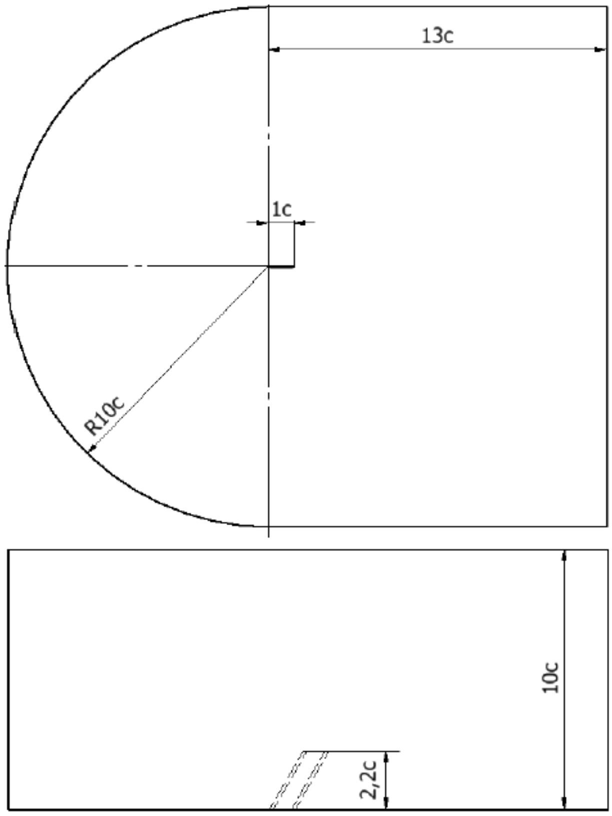

Fig. 9 : Domain of the TM-wing in Edge.

5 Aeroelastic Modelling

The structural and aerodynamic solvers were strongly coupled as part of a partitioned aeroelastic solver implemented in MATLAB. The same spatial discretization of the fin was used for both the structural and aerodynamic solvers, and as such, no interpolation of loads and displacements was necessary for the given geometry and panelling.

The aeroelastic system of equations was formulated in the modal order, with

$$\mathbf{M_{str}}\ddot{x} + \mathbf{C_{str}}\dot{x} + \mathbf{K_{str}}x = Q \tag{13}$$

where the subscript str refers to structural parameters, $\mathbf{M}$ is the mass matrix, $\mathbf{C}$ is the damping matrix, $\mathbf{K}$ is the stiffness matrix, x is the vector of modal displacements, the dot notation referes to differentiation with respect to time, and Q is the vector of generalized aerodynamic forces (GAFs). The aeroelastic equations were solved using the nonlinear formulation of GAFs described in Eqn. 13.

The equations were also solved with the GAFs linearized about trim conditions - this allowed the aerodynamic stiffness and damping matrices to be determined, and rendered the aeroelastic equations linear time invariant (LTI). This formulation is given as

$$\mathbf{M_{ae}}\ddot{x} + \mathbf{C_{ae}}\dot{x} + \mathbf{K_{ae}}x = Q_{offset} \tag{14}$$

where the subscript ae refers to coupled aeroelastic parameters and Q_{offset} represents the offset GAFs associated with the linearization point.

Solution of the nonlinear formulation of Eqn. 13 was accomplished by implicit time-marching using the Newmark-β scheme [16] with

$$\gamma = 1/2 \tag{15}$$

$$\beta = 1/4 \tag{16}$$

$$\Delta t = \frac{T_{min}}{\pi^2} \tag{17}$$

where γ and β are parameters of the algorithm, Δt is the time-step size, and T_{min} is the shortest modal period of the truncate mode set considered (the period of mode 6 was used).

The given set of parameters for the Newmark-β scheme render the scheme unconditionally stable and do not introduce numerical damping [16].

The solution of the LTI system of aeroelastic equations of Eqn. 14 was through eigenanalysis and explicit time-marching using the Runge-Kutta (4,5) integration of the `ode45` function in MATLAB. The time-marching was performed for the state-space formulation of Eqn. 14, given as

$$\begin{Bmatrix} \ddot{x} \\ \dot{x} \end{Bmatrix} = \begin{bmatrix} -\mathbf{M_{ae}^{-1}C_{ae}} & -\mathbf{M_{ae}^{-1}K_{ae}} \\ \mathbf{I} & \mathbf{0} \end{bmatrix} \begin{Bmatrix} \dot{x} \\ x \end{Bmatrix} + \begin{Bmatrix} Q_{offset} \\ 0 \end{Bmatrix} \tag{18}$$

The aeroelastic modelling in Edge coupled the transient Euler solution with a linear modal structural model, with time-averaging of the displacements and GAFs [17]. Post-processing of the modal displacements was performed in MATLAB, and an autoregressive moving-average (ARMA) model of order (4,1) was contructed using the `armax` function in MATLAB for system identification.

The aeroelastic system was perturbed from the trim conditions by setting a small initial disturbance to the displacement of the 2nd mode (first twisting mode).

6 Application

The wind-tunnel flutter test of Torii [15] and Matsuzaki [18] was computationally modelled using the developed aeroelastic prediction tool, with further validation performed through modelling in Edge [5]. Good agreement was obtained with the experimental results, as shown in Table 2.

Table 2: TM-wing flutter dynamic pressures

Analysis Method	q_F [kPa]	%Error
Exp. [15]	113.5	N/A
Edge	108.3	-4.6%
SE/LPT (nonlinear)	120.8	+6.4%
SE/LPT (linear)	124.5	+9.7%
SHABP/LPT (linear)	117.9	+3.9%

As seen from the approximate computational times required (8-core AMD FX-8150 3.6GHz processor, 8GB RAM, and Microsoft Windows 7) for the aeroelastic analysis of one set of flight conditions in Table 3, the use of approximate steady aerodynamic methods (such as shock expansion theory) together with LPT allows for drastic reduction in the computational expense of the analysis. This may be seen to be an extension of the findings of Zhang et al [11] to analytical aerodynamic models, and differs from the work of Liu et al [8] in the use of LPT and the resulting modularity in the steady aerodynamic method.

Table 3: Approximate computation times

Analysis Method	Time	Remarks
Edge	7 hrs	1500 iterations
SE/LPT (nonlinear)	9 hrs	1500 iterations
SE/LPT (linear)	3 min	20x44 mesh
SHABP/LPT (linear)	5 min	10x26 mesh

Whilst higher-fidelity steady aerodynamic analysis (such as Euler or Navier-Stokes computations) offers greater accuracy and solution of the flowfield, it is seen that the zero-order aeroelastic prediction based on computationally inexpensive aerodynamic methods is capable of correctly capturing the physics of fin flutter. The frequency trends with dynamic pressure predicted by SE/LPT shown in Fig. 10 correctly show the coalescence of the first bending (mode 1) and first twisting modes (mode 2) as flutter is approached.

Similarly, the damping trends of the TM-wing shown in Fig. 11 reflect the very sharp decrease in damping of the first twisting mode (mode 2) just prior to flutter. The hard flutter of the TM-wing as reported by Matsuzaki [18] is predicted, although the flutter dynamic pressure is over-predicted by SE/LPT; nonetheless, the flutter type is correctly modelled for negligible computational cost. This allows for informed decisions to be made regarding flutter testing and computation using higher-fidelity, computationally expensive methods.

The frequency trends for the TM-wing predicted by the various computational methods are shown in Fig. 12. The impact of linearizing the GAFs for the given setup may be considered negligible, given the substantial reduction in computational expense.

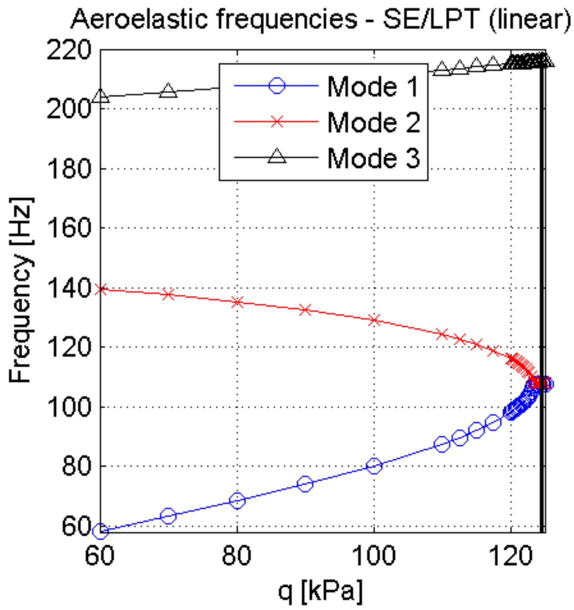

Fig. 10 : TM-wing frequency trends.

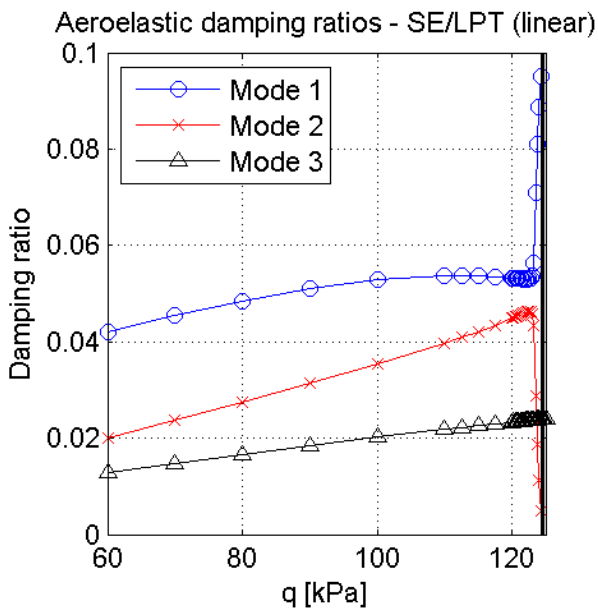

Fig. 11 : TM-wing damping trends.

The linearization of the GAFs in the SE/LPT model allows for rapid assessment of the aeroelastic system parameters. The LTI system offers the further advantage of being suitable for flutter prediction by the Zimmerman-Weissenberger (Z-W) flutter margin [15]. The trend of the Z-W flutter margin with dynamic pressure for the TM-wing is shown in Fig. 13.

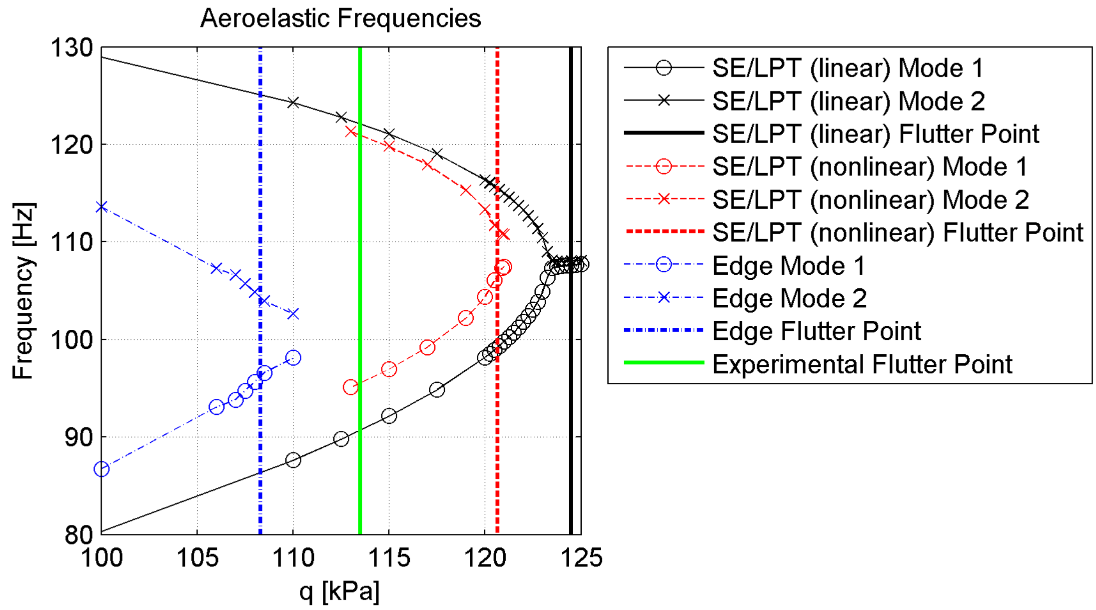

Fig. 12 : Comparison of flutter dynamic pressures.

The very-nearly linear behaviour of the Z-W flutter margin, in conjuction with the LTI system modelled using SE/LPT, allows for the very rapid estimation of the flutter dynamic pressure.

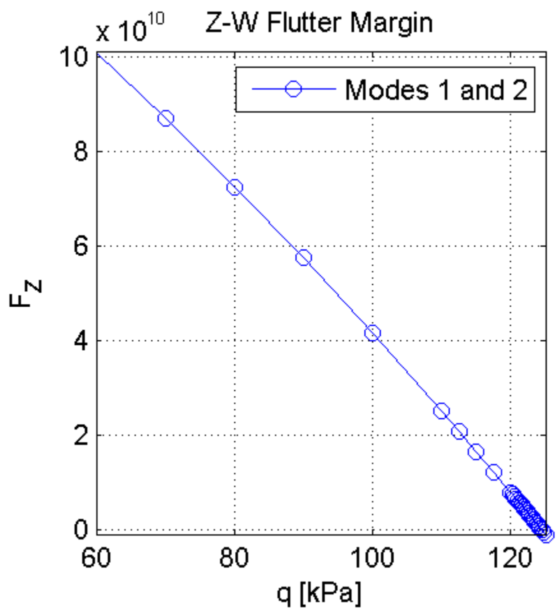

Fig. 13 : Zimmerman-Weissenberger flutter margin.

7 Conclusions

Aeroelastic modelling of lifting surfaces in supersonic flows may be performed using a variety of analysis codes, most of which are commercially available. Local piston theory had previously been shown by Zhang et al [11] to significantly reduce the computational expense of high-fidelity aeroelastic analysis, whilst retaining high solution accuracy. Meijer [5] demonstrated the use of local piston theory with computationally inexpensive aerodynamic methods to be suitable for implementation in a zero-order aeroelastic prediction method. Validation [5] of the prediction method by CFD modelling and by the experimental results of Torii [15] and Matsuzaki [18] showed that accurate predictions could rapidly be made using zero-order methods. Preliminary integration of SHABP with the prediction method by Meijer was successful, and suggested that further integration would result in extension of the SHABP modelling capabilites to aeroelastic prediction for missile fins.

Acknowledgements

The author thanks Armscor for the financial support of this research through the Fluxion grant, and thanks the CSIR for allowing the author the use of Edge.

References

[1] Chabalko, C.C. *Identification of transient nonlinear aeroelastic phenomena*. PhD thesis, Virginia Polytechnic Institute and State University, 2007.

[2] Zona Technology Inc., *http://www.zonatech.com/*, last accessed 26 June 2014.

[3] FreeCASE, *http://www.aero.polimi.it/freecase*, last accessed 26 June 2014.

[4] Dowell, E.H. and Bliss, D.B. New look at unsteady supersonic potential flow aerodynamics and piston theory. *AIAA Journal*, Vol. 51, No. 9, pp 2278-2281, 2013.

[5] Meijer, M.-C. *Aeroelastic prediction methods in supersonic flows for missile design*. MSc dissertation, University of the Witwatersrand, 2014.

[6] Lighthill, M.J. Oscillating airfoils at high Mach number. *Journal of the Aeronautical Sciences*, Vol. 20, No. 6, pp 402-406, 1953.

[7] Ashley, H. and Zartarian, G. Piston theory - a new aerodynamic tool for the aeroelastician. *Journal of the Aeronautical Sciences*, Vol. 23, No. 12, pp 1109-1118, 1956.

[8] Liu, D.D., Yao, Z.X., Sarhaddi, D., and Chavez, F. From piston theory to a unified hypersonic-supersonic lifting surface method. *Journal of Aircraft*, Vol. 34, No. 3, pp 304-312, 1997.

[9] Van Dyke, M.D. A study of second-order supersonic-flow theory. *NACA TN-2200*, 1951.

[10] Donov, A.E. A flat wing with sharp edges in a supersonic stream. *NACA TM-1394*, 1956.

[11] Zhang, W.-W., Ye, Z.-Y, Zhang, C.-A., and Liu, F. Supersonic flutter analysis based on a local piston theory. *AIAA Journal*, Vol. 47, No. 10, pp 2321-2328, 2009.

[12] McNamara, J.J., Crowell, A.R., Friedmann, P.P., Glaz, B. and Gogulapati, A. Approximate modeling of unsteady aerodynamics for hypersonic aeroelasticity. *Journal of Aircraft*, Vol. 47, No. 6, pp 1932-1945, 2010.

[13] Abbas, L.K., Rui, X., Marzocca, P., Abdalla, M., and De Breuker, R. A parametric study on supersonic / hypersonic flutter behavior of aero-thermo-elastic geometrically imperfect curved skin panel. *Acta Mechanica*, Vol. 222, No. 1-2, pp 41-57, 2011.

[14] Yang, C., Li, G. and Wan, Z. Aerothermal-aeroelastic two-way coupling method for hypersonic curved panel flutter. *Science China Technological Sciences*, Vol. 55, No. 3, pp 831-840, 2012.

[15] Torii, H. The extension of discrete-time flutter margin. *28th International Congress of the Aeronautical Sciences*, Brisbane, 2012.

[16] Katona, M.G., Thompson, R. and Smith, J. Efficiency study of implicit and explicit time integration operators for finite element analysis. Civil Engineering Laboratory, *TR-856*, AD A043968, 1977.

[17] *Edge - Theoretical Formulation*, FOI, March 2007, *http://www.foi.se/edge*, last accessed 26 June 2014.

[18] Matsuzaki, Y. Glaz, B. and Gogulapati, A. An overview of flutter prediction in tests based on stability criteria in discrete-time domain. *Internation Journal of Aeronautical and Space Sciences*, Vol. 12, No. 4, pp 305-317, 2011.

Copyright Statement

The authors confirm that they, and/or their company or organization, hold copyright on all of the original material included in this paper. The authors also confirm that they have obtained permission, from the copyright holder of any third party material included in this paper, to publish it as part of their paper. The authors confirm that they give permission, or have obtained permission from the copyright holder of this paper, for the publication and distribution of this paper as part of the ICAS 2014 proceedings or as individual off-prints from the proceedings.